The Track Integrated Kinetic Energy of Atlantic Tropical Cyclones

V. MISRA

Department of Earth, Ocean and Atmospheric Science, and Center for Ocean–Atmospheric Prediction Studies, and Florida Climate Institute, The Florida State University, Tallahassee, Florida

S. DINAPOLI

Center for Ocean–Atmospheric Prediction Studies, The Florida State University, Tallahassee, Florida

M. POWELL

NOAA/Atlantic Oceanographic and Meteorological Laboratory/Hurricane Research Division, Miami, Florida

(Manuscript received 13 December 2012, in final form 6 February 2013)

ABSTRACT

In this paper the concept of track integrated kinetic energy (TIKE) is introduced as a measure of seasonal Atlantic tropical cyclone activity and applied to seasonal variability in the Atlantic. It is similar in concept to the more commonly used accumulated cyclone energy (ACE) with an important difference that in TIKE the integrated kinetic energy (IKE) is accumulated for the life span of the Atlantic tropical cyclone. The IKE is, however, computed by volume integrating the 10-m level sustained winds of tropical strength or higher quadrant by quadrant, while ACE uses the maximum sustained winds only without accounting for the structure of the storm. In effect TIKE accounts for the intensity, duration, and size of the tropical cyclones. In this research, the authors have examined the seasonality and the interannual variations of the seasonal Atlantic TIKE over a period of 22 yr from 1990 to 2011. It is found that the Atlantic TIKE climatologically peaks in the month of September and the frequency of storms with the largest TIKE are highest in the eastern tropical Atlantic. The interannual variations of the Atlantic TIKE reveal that it is likely influenced by SST variations in the equatorial Pacific and in the Atlantic Oceans. The SST variations in the central equatorial Pacific are negatively correlated with the contemporaneous seasonal (June–November) TIKE. The size of the Atlantic warm pool (AWP) is positively correlated with seasonal TIKE.

1. Introduction

The concept of the integrated kinetic energy (IKE) of a tropical cyclone, first introduced by Powell and Reinhold (2007), was motivated by its ability to represent the destructive potential of the storm. Powell and Reinhold (2007) argue that the intensity of the storm as measured by the Saffir–Simpson scale is actually a poor measure of the destructive potential of the storm. This point is illustrated somewhat by the extensive damage in the U.S. Gulf states caused by Katrina in 2005, which was a storm weaker than Camille, which caused far less destruction. More recently Irene in 2011 and Isaac and Sandy in 2012, while relatively weak on the Saffir–Simpson scale, caused considerable damage and mortality. In terms of IKE all of these storms would be rated significantly greater owing to the relatively large extent of the tropical storm winds. As discussed in Powell and Reinhold (2007), kinetic energy scales with the surface stress that forces storm surge and waves, and the horizontal wind loads specified by the American Society of Civil Engineers (ASCE 2005) also scale with kinetic energy, making IKE a relevant metric to represent the destructive potential of the tropical cyclone.

In this paper we extend the concept of IKE by accumulating IKE over the life span of the tropical storm to what we define as the track integrated kinetic energy (TIKE).[1] It is apparent that TIKE has some similarity to

Corresponding author address: V. Misra, Department of Earth, Ocean and Atmospheric Sciences, The Florida State University, 1017 Academic Way, 404 Love Building, Tallahassee, FL 32312.
E-mail: vmisra@fsu.edu

DOI: 10.1175/MWR-D-12-00349.1

[1] See the appendix for the calculation of TIKE.

accumulated cyclone energy (ACE; Bell et al. 2000) and power dissipation index (PDI; Emanuel 2005, 2007) in that all these metrics are integrated over the life span of the tropical storm. ACE and PDI, however, are critically dependent on the intensity with the former using the square and the latter using the cube of the maximum sustained wind measured at 6-h intervals. Furthermore, Yu et al. (2009) and Yu and Chiu (2012) suggest that ACE inordinately overestimates the energy of the tropical cyclones in comparison to IKE as it does not take into account the structure of the cyclone. In fact they suggest the discrepancy between IKE and ACE increases exponentially with increasing maximum sustained winds of the tropical cyclone. As discussed in Powell and Reinhold 2007, this maximum sustained wind is the highest 1-min-average wind measured at 10 m above the surface with unobstructed exposure (National Weather Service 2006). Obviously this quantity is rarely measured directly. It is often estimated empirically from flight level reconnaissance wind measurements (Franklin et al. 2003). Other alternative measures like using satellite imagery (Dvorak 1975) or pressure–wind relationship (Kraft 1961) are also used to estimate the wind intensity of the tropical storms in the prereconnaissance period. However, both PDI and ACE are known to ignore the spatial distribution of these strong winds, which is argued to be critical in assessing the destructive potential of landfalling tropical cyclones (Powell and Reinhold 2007). Therefore, the motivation of this paper is to understand the seasonal Atlantic tropical cyclone activity in terms of the accumulated IKE of the observed storms.

2. Methodology

We calculate TIKE for each named system in the Atlantic hurricane basin from 1990 through 2011 by summing the IKE values every 6 h over the lifetime of the storm. IKE is computed using wind speed and radii data from the Colorado State University Extended Best Track dataset (Demuth et al. 2006). This dataset is presently available from 1988 through 2011, but the data in 1988 and 1989 are incomplete and are therefore not included in our analysis. The wind radii are based on the National Hurricane Center's poststorm estimates from 2004 onward and on operational estimates prior to 2004. Therefore, interpretation of interannual and longer variability of TIKE has to be done with caution since year to year changes are subject to variations of data quality and quantity.

IKE is calculated for each Atlantic tropical cyclone at 6-h intervals at which the storm has maximum sustained winds of 34 kt ($\sim$17.5 m s^{-1}) or greater, provided that operational or poststorm data are available. There

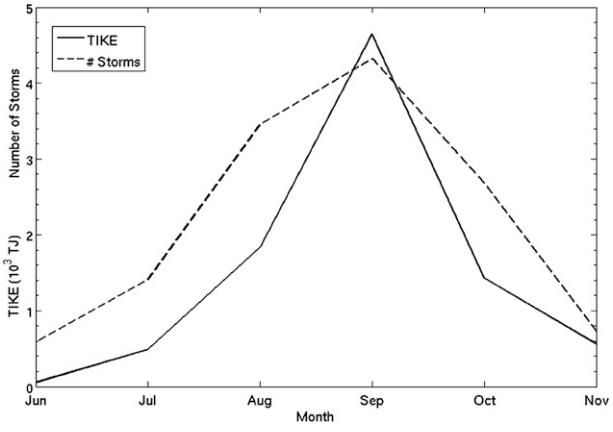

FIG. 1. Climatological values of TIKE and number of storms for each month of the year.

are a few occasions in which wind radii data are unavailable; this primarily occurs in storms that were not monitored operationally and were discovered in postseasonal analysis. We believe omitting these cases will have a negligible impact on the results because of the weakness and short duration of such storms. We also note that IKE is designed as an indicator of a storm's destructive potential (Powell and Reinhold 2007), and, therefore, does not account for wind speeds below tropical storm strength.

The formulas to calculate IKE from the wind radii data were originally published by Powell and Reinhold (2007), however, these formulas were based on radii from the Hurricane Research Division (HRD) Real-time Hurricane Wind Analysis System (H*Wind). Operational wind radii tend to be smaller than those from H*Wind (Moyer et al. 2007), and, therefore, we utilize new formulas described in the appendix. These formulas calculate kinetic energy by using an estimation of the mean wind between each operational quadrant wind radius. The kinetic energy is then integrated over the area to obtain IKE.

3. Results

a. Seasonal climatology

It is well known that the seasonal peak of genesis for Atlantic tropical cyclones is in the month of September (Gray 1968; Fig. 1). The TIKE also coincides with this peak in September (Fig. 1). When we examine the distribution of the median radius of each tropical cyclone forced with at least tropical storm–strength winds, September seems to show the highest frequency of larger radii storms (Fig. 2a). Therefore, the peak in TIKE (Fig. 1) is associated with a corresponding peak in larger

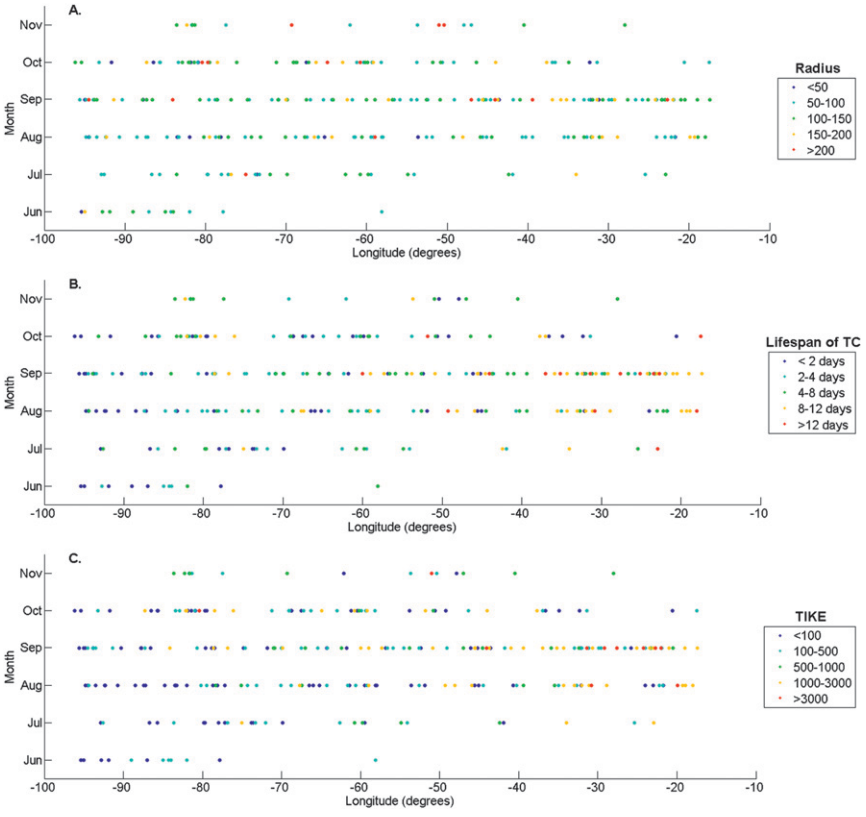

FIG. 2. Scatterplot showing the month and longitude of formation for all storms used in the TIKE calculations. The following are calculated based on tropical cyclones used in the calculation of TIKE in Fig. 1. Storms are color coded based on (a) the median radius (defined over the life span of each tropical cyclone used in the calculation of TIKE in Fig. 1) in nautical miles, (b) the length of time over which IKE was integrated, and (c) the value of TIKE (TJ).

sized storms in September. Another important factor that enters in the calculation of TIKE is the length of time during which the tropical cyclone maintains winds of at least tropical storm force. Figure 2b shows the distribution of the length of the time over which IKE is integrated. Again we see that the longest-lived cyclones in the Atlantic with at least tropical storm–forced wind appear most frequently in September. Therefore, the climatological peak of TIKE in September is also associated with the longer-lived tropical storms.

In Figs. 2a,b it is also apparent that these large-sized and long-lived storms make their genesis to form in the east Atlantic (east of 50°W). As a result it is expected that the frequency of high TIKE Atlantic storms will be more in the east Atlantic (Fig. 2c). However, in Fig. 2c, October shows a spike in high TIKE cyclones west of 50°W that is coincident with a corresponding notable increase in cyclones with radii greater than 150 km (Fig. 2a) and with a life span of more than 4 days (Fig. 2b).

b. Interannual variability

The seasonal TIKE exhibits significant interannual variations, which is comparable to other metrics that measure the seasonal Atlantic tropical cyclone activity (e.g., ACE, PDI, number of Atlantic storms; Fig. 3a). The correlations between TIKE and ACE is 0.86, TIKE and the number of storms is 0.61, and between ACE and the number of storms is 0.78 (Fig. 3a). In fact we contend that the interannual variations of TIKE in comparison to the other two metrics are quite illuminating (Fig. 3a). For example, in the 2005 seasons there were 28 named tropical Atlantic cyclones, a highly anomalous year in terms of this metric and even ACE (Fig. 3a). However, TIKE proved to be far less in magnitude suggesting that 2005 season was not as anomalous. In other words, this comparison reveals that 2005 was not characterized by as many large-sized and long lived storms as other active seasons, such as 1995. In terms of the most anomalous seasons with high (low) TIKE 1995 (1993) followed by 1999 (1991) stand out.

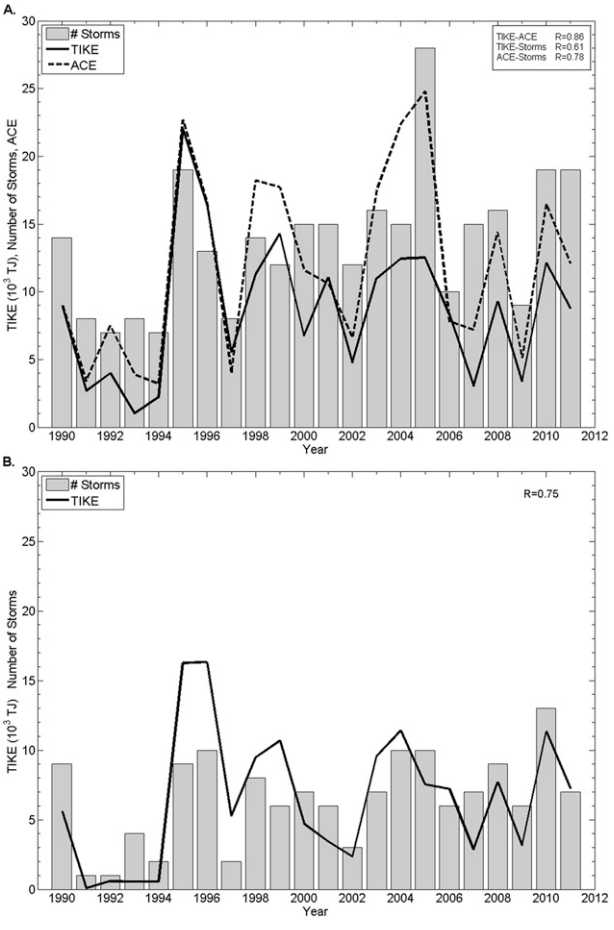

FIG. 3. (a) Total values of TIKE, ACE, and the number of storms for each year from 1990 to 2011, and (b) TIKE and the number of storms originating in the MDR region only. (top right) The contemporaneous correlation coefficients between these metrics are shown.

Figure 3b shows the interannual variations of the seasonal TIKE, ACE, and the number of storms that formed in the Maximum Development Region (MDR; 10°–20°N, 80°–20°W) only. Here the TIKE and number of storms are more similar than over the entire Atlantic basin. Moreover the 2005 season does not appear to be the most anomalous years in all three metrics (Fig. 3b). In comparison to Fig. 3a, a majority of the 2005 storms formed northwest of the MDR. Thus, many of these storms had insufficient time to remain over warm water to develop large TIKE before either making landfall or transitioning to post-tropical storms.

c. *Relationship with SST variations*

Figure 4a shows the contemporaneous correlations of TIKE with global SST. The appearance of the negative correlations with the central and eastern Pacific SST anomalies points to the well-known ENSO teleconnection. Figure 4a reveals that higher seasonal TIKE is associated with the cold phase of ENSO and warm SSTs in the tropical and higher-latitude Atlantic Ocean. It is interesting to note, however, that the statistically significant correlations in the Pacific are more apparent in the central equatorial Pacific region, suggesting the possible influence of the Modoki El Niño (Ashok et al. 2007; Ashok and Yamagata 2009; Kao and Yu 2009). Modoki (or central Pacific) El Niño unlike the traditional (or east Pacific) El Niño has its largest SST anomalies in the central (Niño 3.4) Pacific region with insignificant anomalies in the far eastern equatorial (Niño 1+2) Pacific region. It may be mentioned that in recent decades the Modoki El Niño appears to be occurring more frequently than before (Yeh et al. 2009). However, the ACE index shows a broad influence of the equatorial Pacific SST anomalies stretching from the central to the far eastern equatorial Pacific Ocean (Fig. 4b). Figure 4a also shows that while the El Niño–related SST anomalies is associated with the reduction in the seasonal TIKE anomalies, the appearance of warm SST anomalies in the Atlantic is associated with an increase in the seasonal TIKE anomaly.

The remote forcing of the tropical Pacific in the seasonal Atlantic TIKE anomalies stem from the modulation of the vertical wind shear (defined between winds at 850 and 200 hPa). In Fig. 5 we show the correlations of TIKE from storms that make their genesis in the MDR with global vertical wind shear anomalies. In the region of the MDR the seasonal TIKE anomalies are negatively correlated with the wind shear, which is consistent with similar relationships seen in case of ACE and the number of Atlantic tropical cyclone for the season (not shown).

In the tropical Atlantic the larger seasonal TIKE anomalies are also associated with the larger size of the Atlantic warm pool (AWP; Wang and Enfield 2001; Wang et al. 2011) in the August–September–October (ASO) season (a season of annual peak in the size of the AWP). The correlation of ASO AWP size and TIKE is 0.43 (Fig. 6). This relationship is not surprising given that Wang et al. (2011) have already shown that years with large-size AWP are associated with more eastern tropical Atlantic cyclone activity.

4. Summary and conclusions

In this paper we introduce a new metric called the track integrated kinetic energy (TIKE) as a measure for Atlantic tropical cyclone activity. It is not being suggested as an alternative metric but a complimentary one to the existing metrics. ACE for example, emphasizes on the intensity of the storm and PDI overemphasizes on the maximum sustained surface winds, being proportional

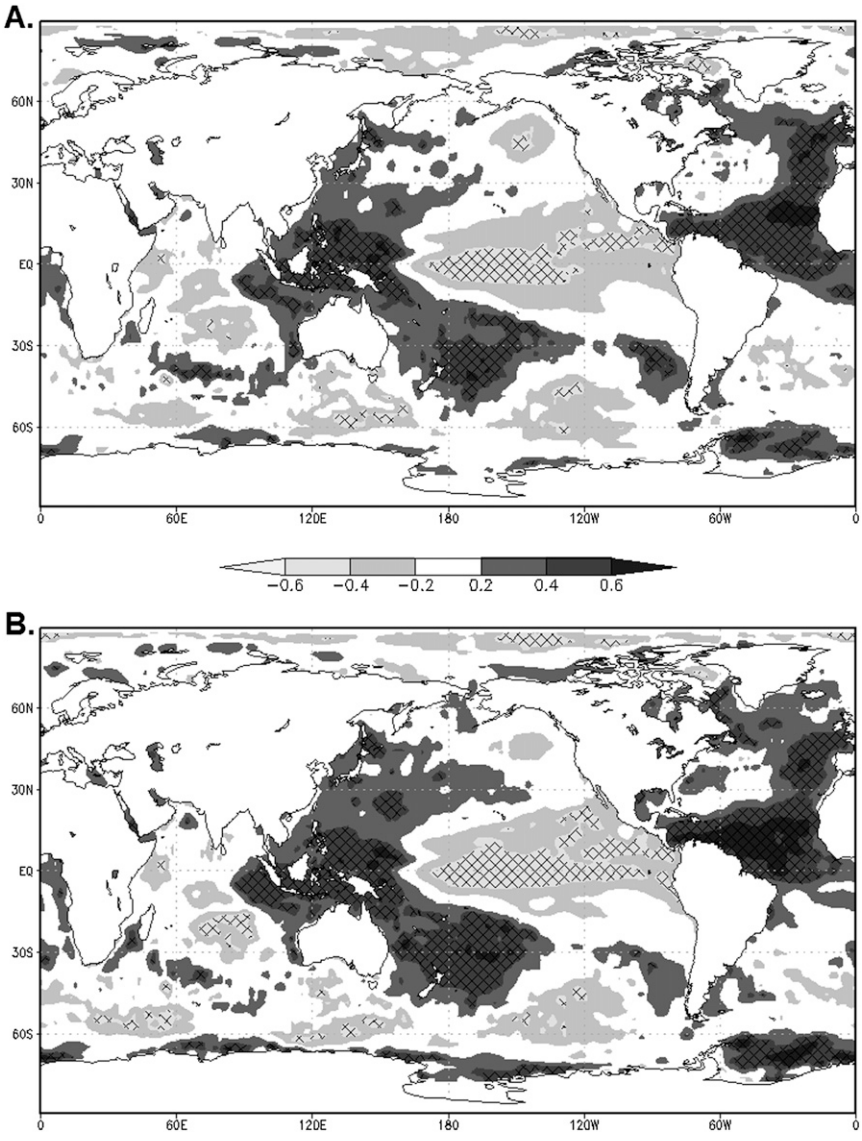

FIG. 4. Correlation of (a) total TIKE and (b) ACE with contemporaneous SST from version 2 of the optimum interpolation sea surface temperature (OISSTv2) analysis. Hashing shows significance at the 95% confidence interval.

to its third power. The number of storms in the season, which is reasonably well predicted a season in advance (LaRow et al. 2010; LaRow 2013) is another metric in common use to measure the seasonal activity of the tropical Atlantic storms. The TIKE, which is the accumulation of the integrated kinetic energy (IKE) for the life span of the tropical cyclone, is a measure of intensity, size, and duration.

Our analysis reveals that the TIKE metric further illuminates on the seasonal activity of the Atlantic tropical storms. For example, the 2005 season, while quite anomalous both in terms of ACE and number of storms, did not stand out as significantly anomalous in seasonal TIKE anomaly. This would suggest that the 2005 season was not characterized by many large and long-lasting storms. However the 1995 (1993) season was anomalously high (low) in all three metrics.

The climatology of TIKE is similar to the other metrics in that it exhibits an annual peak in September. This annual peak in TIKE is associated with larger and longer-lasting storms that invariably make genesis in the eastern Atlantic.

The global teleconnections of the seasonal TIKE anomalies expose the usual suspects of El Niño–Southern Oscillation (ENSO) SST anomalies in the tropical Pacific and the northern (tropical and higher latitude) Atlantic

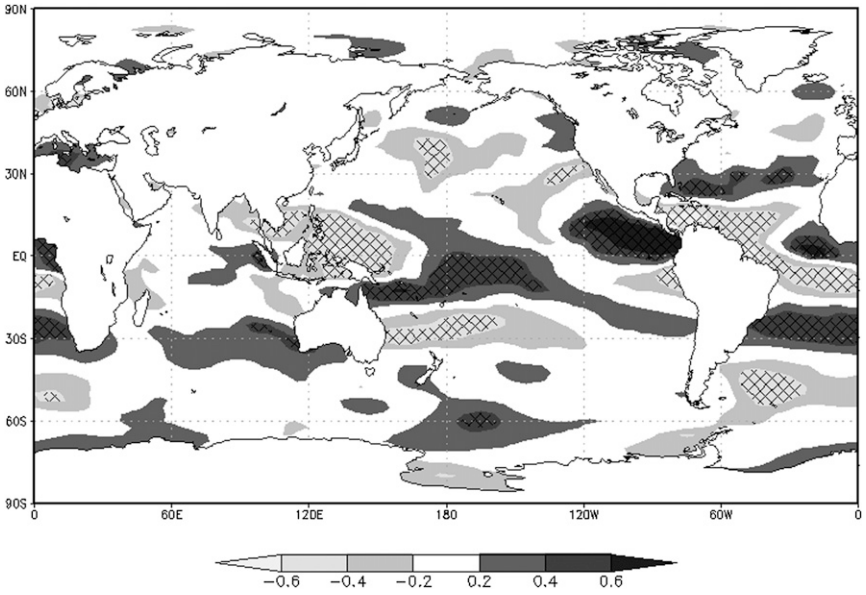

FIG. 5. Contemporaneous correlation of TIKE for storms originating over the MDR region with contemporaneous vertical shear from the National Centers for Environmental Prediction–Department of Energy Global Reanalysis 2 (NCEP R2). Hashing shows significance at the 95% confidence interval.

SST anomalies. A visible subtlety with the teleconnection of the tropical Pacific SST anomalies is that the more significant correlations are in the central Pacific, which possibly suggests the influence of the so-called Modoki El Niño on the seasonal TIKE anomalies.

The AWP size also shows an influence on TIKE with larger size of AWP associated with higher seasonal TIKE anomalies. It is also shown that at least in the last two decades the storms with relatively higher TIKEs have contributed more to the seasonal (June–November) seasonal rainfall.

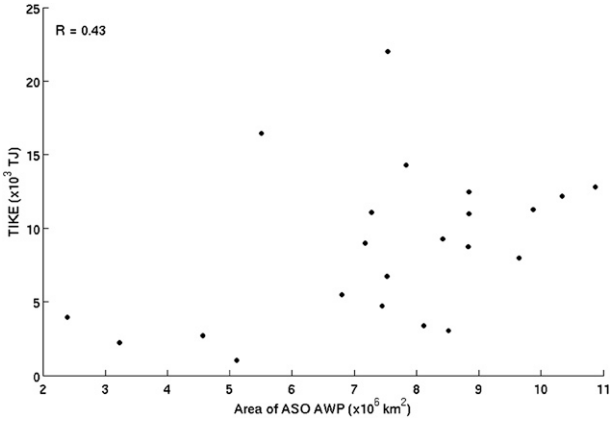

FIG. 6. Scatterplot showing TIKE plotted against the ASO-averaged area of the Atlantic warm pool. (top-left corner) The correlation coefficient is shown.

Generating the values of the TIKE prior to 1990 is a challenge with the absence of the radius of the tropical-forced winds for the Atlantic storms. Likewise, the absence of this data for other tropical ocean basins for as many years as the tropical Atlantic makes it difficult to examine their variations and climatology of TIKE and, hence, the global TIKE.

Acknowledgments. We thank Michael Kozar with assistance in the generation of some of the figures. We would also like to thank one anonymous reviewer and Mike Fiorino for their insightful comments on an earlier version of the manuscript. This work was supported by grants from NOAA (Grants NA12OAR4310078, NA10OAR4310215, and NA11OAR4310110), USGS (Grant 06HQGR0125), and USDA (Grant 027865).

APPENDIX

Calculation of Track Integrated Kinetic Energy (TIKE)

TIKE is a seasonal integration of the integrated kinetic energy (IKE) over all tropical cyclones in a given basin. The IKE is calculated as a volume integral, considering a layer thickness of 1 m centered at the 10-m level:

$$\mathrm{IKE} = \int_v 1/2\rho A V^2, \qquad \text{(A1)}$$

TABLE A1. Guidelines for computing IKE from operational quadrant wind radii. The R_{18}, R_{26}, R_{33}, and R_{max} variables are the radii of 18 m s^{-1}, 26 m s^{-1}, 33 m s^{-1}, and maximum winds, respectively; V_{MS} is the maximum sustained surface wind speed. All radii are measured in meters.

Quadrant IKE contribution	Criteria	Mean wind (m s^{-1})	Area (m^2)
IKE_{18-26}	$R_{26} > 0$	20	$0.25\pi(R_{18}^2 - R_{26}^2)$
	No R_{26}, $V_{MS} > 26$, $R_{18} > R_{max}$	20	$0.25\pi[R_{18}^2 - (0.75R_{max})^2]$
	No R_{26}, $V_{MS} < 26$, $R_{18} > R_{max}$	$0.25V_{MS} + 0.75(18)$	$0.25\pi[R_{18}^2 - (0.75R_{max})^2]$
	No R_{26}, $R_{max} = R_{18}$	18	$0.25\pi[R_{18}^2 - (0.5R_{18})^2]$
IKE_{26-33}	$R_{33} > 0$	27.75	$0.25\pi(R_{26}^2 - R_{33}^2)$
	No R_{33}, $V_{MS} > 33$, $R_{26} > R_{max}$	27.75	$0.25\pi[R_{26}^2 - (0.75R_{max})^2]$
	No R_{33}, $V_{MS} < 33$, $R_{26} > R_{max}$	$0.25V_{MS} + 0.75(26)$	$0.25\pi[R_{26}^2 - (0.75R_{max})^2]$
	No R_{33}, $R_{26} \leq R_{max}$	26	$0.25\pi[R_{26}^2 - (0.5R_{26})^2]$
IKE_H	Max R_{33} quadrant, $R_{33} > R_{max}$	$0.25V_{MS} + 0.75(33)$	$0.25\pi[R_{33}^2 - (0.75R_{max})^2]$
	Max R_{33} quadrant, $R_{33} = R_{max}$	$0.25V_{MS} + 0.75(33)$	$0.25\pi[R_{33}^2 - (0.75R_{33})^2]$
	$R_{33} < R_{max}$	$0.1V_{MS} + 0.9(33)$	$0.25\pi[R_{33}^2 - (0.75R_{33})^2]$
	Not max R_{33} quadrant, $R_{max} = R_{33}$	$0.1V_{MS} + 0.9(33)$	$0.25\pi[R_{33}^2 - (0.75R_{max})^2]$

where ρ is air density, and A and V are, respectively, the area and mean 10-m wind speed of the contributing portion of the quadrant according to Table A1. All quadrant contributions are summed to compute the IKE of the storm.

REFERENCES

ASCE, 2005: ASCE 7-05: Minimum design loads for buildings and other structures. American Society of Civil Engineers, 424 pp.

Ashok, K., and T. Yamagata, 2009: Climate change: The El Niño with a difference. *Nature,* **461,** 481–484.

——, S. K. Behera, S. A. Rao, H. Weng, and T. Yamagata, 2007: El Niño Modoki and its possible teleconnection. *J. Geophys. Res.,* **112,** C11007, doi:10.1029/2006JC003798.

Bell, G. D., and Coauthors, 2000: Climate assessment for 1999. *Bull. Amer. Meteor. Soc.,* **81,** S1–S50.

Demuth, J. L., M. DeMaria, and J. A. Knaff, 2006: Improvement of advanced microwave sounder unit tropical cyclone intensity and size estimation algorithms. *J. Appl. Meteor. Climatol.,* **45,** 1573–1581.

Dvorak, V. F., 1975: Tropical cyclone intensity analysis and forecasting from satellite imagery. *Mon. Wea. Rev.,* **103,** 420–430.

Emanuel, K., 2005: Increasing destructiveness of tropical cyclones over the past 30 years. *Nature,* **436,** 686–688.

——, 2007: Environmental factors affecting tropical cyclone power dissipation. *J. Climate,* **20,** 5497–5509.

Franklin, J. L., M. L. Black, and K. Valde, 2003: GPS dropwindsonde wind profiles in hurricanes and their operational implications. *Wea. Forecasting,* **18,** 32–44.

Gray, W. M., 1968: Global view of the origins of tropical disturbances and storms. *Mon. Wea. Rev.,* **96,** 669–700.

Kao, J.-Y., and J.-Y. Yu, 2009: Contrasting eastern Pacific and central Pacific types of ENSO. *J. Climate,* **22,** 615–632.

Kraft, R. H., 1961: The hurricane's central pressure and highest wind. *Mar. Wea. Log.,* **5,** 155.

LaRow, T. E., 2013: The impact of SST bias correction on North Atlantic hurricane retrospective forecasts. *Mon. Wea. Rev.,* **141,** 490–498.

——, L. Stefanova, D. W. Shin, and S. Cocke, 2010: Seasonal Atlantic tropical cyclone hindcasting/forecasting using two sea surface temperature datasets. *Geophys. Res. Lett.,* **37,** L02804, doi:10.1029/2009GL041459.

Moyer, A. C., J. L. Evans, and M. Powell, 2007: Comparison of observed gale radius statistics. *Meteor. Atmos. Phys.,* **97,** 41–55.

National Weather Service, 2006: Tropical cyclone definitions. National Weather Service Manual 10-604, 12 pp. [Available online at http://www.nws.noaa.gov/directives/010/010.htm.]

Powell, M. D., and T. A. Reinhold, 2007: Tropical cyclone destructive potential by integrated kinetic energy. *Bull. Amer. Meteor. Soc.,* **88,** 513–526.

Wang, C., and D. B. Enfield, 2001: The tropical Western Hemisphere warm pool. *Geophys. Res. Lett.,* **28,** 1635–1638.

——, H. Lui, S. Lee, and R. Atlas, 2011: Impact of the Atlantic warm pool on United States landfalling hurricanes. *Geophys. Res. Lett.,* **38,** L19702, doi:10.1029/2011GL049265.

Yeh, S.-W., J.-S. Kug, B. Dewitte, M.-H. Kwon, B. P. Kirtman, and F.-F. Jin, 2009: El Niño in a changing climate. *Nature,* **461,** 511–514.

Yu, J.-Y., and P.-G. Chiu, 2012: Contrasting various metrics for measuring tropical cyclone activity. *Terr. Atmos. Oceanic Sci.,* **23,** 303–316.

——, C. Chou, and P.-G. Chiu, 2009: A revised accumulated cyclone energy index. *Geophys. Res. Lett.,* **36,** L14710, doi:10.1029/2009GL039254.